



Compression-Driven Mass Flow in Bulk Solid ^4He

Zhi Gang Cheng and John Beamish

Department of Physics, University of Alberta, Edmonton, Alberta, Canada T6G 2E1

(Received 18 February 2016; published 6 July 2016)

Mass flow has been observed in solid ^4He coexisting with superfluid confined in Vycor, but its physical mechanism remains an open question. Here we report observations of flow in experiments in which Vycor has been eliminated, allowing us to study the intrinsic flow in solid ^4He without the complications introduced by the presence of superfluid and the associated solid-liquid interfaces. By growing crystals with ^3He concentration as low as $x_3 = 5 \times 10^{-12}$, we also avoided the low temperature flow suppression observed in previous experiments and found that the flow rate continued to increase down to at least 28 mK without saturation. In addition, ^3He concentrations of 120 ppb, which suppressed most of the low temperature flow in previous experiments, had no effect in our samples. The larger ^3He concentrations needed to block the bulk solid flow suggest that the mass flow involves a larger area, such as disordered liquid layer on solid surface and grain boundaries.

DOI: [10.1103/PhysRevLett.117.025301](https://doi.org/10.1103/PhysRevLett.117.025301)

Solid helium is a uniquely quantum material with unusual behavior at low temperatures, the most spectacular prediction being supersolidity [1–3]. Torsional oscillator experiments on solid ^4He [4,5] appeared to show evidence of supersolid mass decoupling, but these now appear to be artifacts of elastic effects in the helium [6–8]. Recently, however, mass flow was observed in experiments in which solid ^4He was sandwiched between two “superfluid leads” [9,10]. These were made of Vycor glass, whose small pores suppressed freezing so that the helium remained liquid at pressures well above the bulk melting curve [11]. The flow in this “liquid-solid-liquid” (LSL) junction was only observed for samples with pressure lower than 28 bar and at temperatures below 600 mK. The flow rate increased with decreasing temperature but was rapidly suppressed below a temperature T_{onset} (~ 100 mK), which depended on the ^3He concentration x_3 . The flow was interpreted in terms of a network of dislocations whose cores could be superfluid or form a one-dimensional Luttinger liquid. The drop at T_{onset} could be due to ^3He impurities binding to dislocations and disrupting the flow. However, the interpretation of these measurements is complicated by the fact that the flow must pass through bulk solid, superfluid in the Vycor leads, and two solid-liquid interfaces at the Vycor surfaces, any of which could limit the flow. The observation of flow certainly shows that mass can be transported through a solid ^4He channel, and the universal temperature dependence of the measured flow rate is a strong argument that it is a property of the solid itself. In more recent experiments, we generated mass flow through a Vycor superfluid channel by mechanical compression of solid helium at one end of a “solid-liquid-solid” (SLS) junction [12]. The dependence on temperature was essentially the same as in the LSL junction measurements, as was the suppression by ^3He . However, as we argued in that Letter, the low

temperature flow suppression by ^3He impurities reflects a bottleneck at the solid-liquid interfaces where ^3He is tightly bound and accumulates at low temperatures, rather than the effect of ^3He on the flow within the solid ^4He .

Recent measurements in the LSL geometry have shown that pressure gradients in the solid can relax at low temperatures, even without flow through the superfluid leads [13]. These experiments did not vary the ^3He concentration or extend to low enough temperatures to observe flow suppression and so could not address the question of where the ^3He blocks the flow at low temperatures. Even in these experiments, the presence of Vycor may be important, since ^3He is more strongly bound in the liquid so its concentration in the solid varies with temperature and is greatly reduced at low temperatures [12].

In this Letter, we describe flow through bulk solid ^4He samples where there are no complications from Vycor superfluid channels or solid-liquid interfaces. We measured the flow in crystals of extremely high isotopic purity, at temperatures as low as 28 mK. As in previous experiments, the flow appeared below 600 mK and increased with decreasing temperature. In the samples grown from gas with ^3He concentration $x_3 = 5 \times 10^{-12}$ (5 ppt) and $x_3 = 1.2 \times 10^{-7}$ (120 ppb), we saw no suppression related to ^3He , allowing us to study the intrinsic bulk solid flow to our lowest temperatures. At higher x_3 (up to 1500 ppm) the flow was suppressed at low temperatures, but the amount of ^3He needed to block the flow was much larger than in previous experiments [10,12], suggesting that the flow blockage involves a larger region, which may include a disordered layer at the cell walls, and grain boundaries in polycrystalline samples.

A schematic drawing of our experimental cell (Fig. 1) shows two thin disk-shaped chambers connected by a

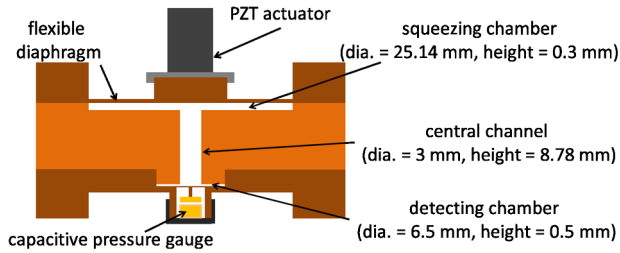


FIG. 1. Schematic cross section of the cell. The sample space has a volume of 227.6 mm^3 and surface area of 1161.7 mm^2 .

cylindrical flow channel. The top of the upper (squeezing) chamber is a 0.8 mm thick flexible diaphragm, allowing us to compress the solid helium. The bottom of the lower (detecting) chamber is the 0.3 mm thick diaphragm of a capacitive pressure gauge. All samples were polycrystals, prepared using the blocked-capillary method. As in previous experiments [12], solid helium was squeezed by applying a dc voltage to a lead zirconate titanate (PZT) actuator [14] rigidly mounted against a “compression button” at the center of the diaphragm. The displacement d_0 at the center of the diaphragm was calibrated at 3.3 nm/V [12].

We first made a sample at 26.5 bar using isotopically purified helium gas with $x_3 = 5 \text{ ppt}$ [15]. Figure 2(a) shows the pressure response in the detecting chamber when the helium in the squeezing chamber was compressed

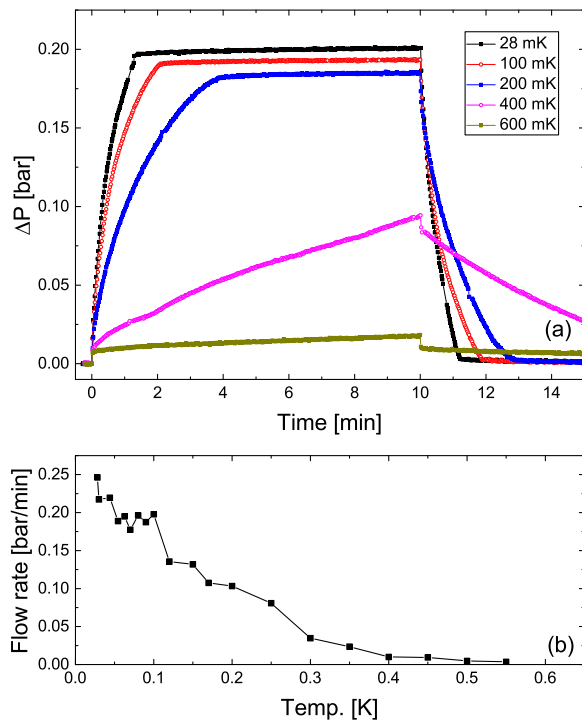


FIG. 2. (a) Pressure responses at different temperatures for the 5 ppt sample. The elastic response is independent of temperature, while the mass flow rate is temperature dependent. (b) Intrinsic temperature dependence of flow rate.

by a $d_0 = 1.0 \mu\text{m}$ displacement of the diaphragm. At each temperature, squeezing produced an immediate pressure jump of $\sim 8 \text{ mbar}$ (most obvious in the 600 mK data), which reversed when the compression was released after 10 min . This is the result of elastic deformation of the helium in the flow channel [16], not of flow through the channel. Following the elastic jump, the pressure rises more slowly but stops abruptly after a few minutes ($\sim 1 \text{ min}$ at 28 mK , more than 10 min above 400 mK). This is in contrast to the exponential pressure relaxation that is seen for viscous flow or at temperatures near melting where thermally activated diffusion is possible [12,17]. We characterized the flow rate by a linear fit of the initial 25% of the pressure rise. The temperature dependence of this flow is shown in Fig. 2(b). Flow appeared below 600 mK and increased down to the lowest temperature, 28 mK . Mass flow was seen in about half of the samples at pressures below about 28 bar but never seen at higher pressures. In the samples with flow, the temperature dependence was consistent, but the magnitude of the flow varied between samples and sometimes changed when a sample was thermally cycled up to $\sim 600 \text{ mK}$. These variations may be due to randomness and annealing effects in the surfaces and grain boundaries of our polycrystalline samples.

In addition to the 5 ppt sample, we grew crystals with higher ^3He concentrations: $x_3 = 120 \text{ ppb}$, 20 ppm , 200 ppm , and 1500 ppm . The 120 ppb sample used commercial ^4He gas and the other samples were made by adding ^3He to the empty cell before filling it with commercial ^4He . Figure 3 shows the temperature dependence of the flow rate in samples with these concentrations. The magnitudes of the flow (shown in the inset of Fig. 3) were sample dependent, but the temperature dependence was essentially the same, as can be seen in the normalized data of Fig. 3. Compared to LSL and SLS experiments,

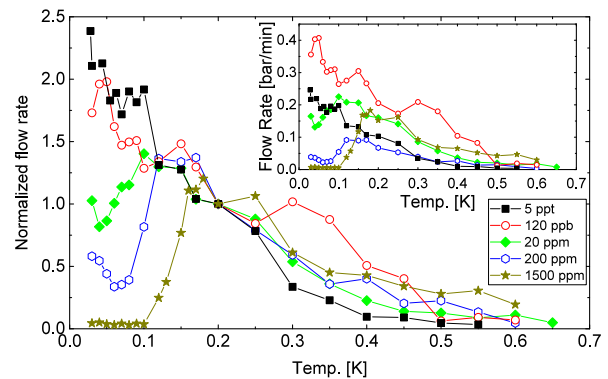


FIG. 3. Temperature dependence of normalized flow rates for samples with $x_3 = 5 \text{ ppt}$, 120 ppb , 20 ppm , 200 ppm , and 1500 ppm , and pressure at 26.5 , 25.9 , 26.0 , 25.9 , and 26.3 bar , respectively. The data are normalized by the flow rate at 0.2 K . Inset: Temperature dependence of flow rates without normalization.

much more ^3He was needed to suppress the flow. We saw no low temperature flow drop in the 120 ppb sample. A drop was observed below 100 mK for the 20 ppm sample, but the maximum suppression was only $\sim 40\%$ at 40 mK. A sharper drop was observed below 120 mK for the 200 ppm sample with a maximum suppression of $\sim 75\%$. Only in the 1500 ppm sample was the flow completely suppressed below 100 mK.

We were also able to measure the ac pressure response P_{ac} when a low frequency voltage $V(t) = V_0 \sin(2\pi ft)$ was applied to the PZT actuator. P_{ac} is not a direct measurement of the flow rate, but, as discussed in Supplemental Material [16], higher flow rates generate larger values of P_{ac} , providing the ac frequency is chosen appropriately. Figure 4 shows the temperature dependence of the magnitude and phase of P_{ac} for the 5 ppt, 200 ppm, and 1500 ppm samples, measured at a frequency of 0.02 Hz. The overall behavior observed in the dc measurements is reproduced in the ac results, but with less scatter because of the averaging inherent in the ac measurement.

The ac pressure response is a combination of elastic deformation and mass flow. The elastic response is nearly independent of temperature and occurs on millisecond time scales, much faster than the period of the 0.02 Hz ac drive, so its magnitude P_{ac} is constant and the phase lag $\Delta\phi$ is essentially zero. The orange symbols in Fig. 4, for a sample which did not show any flow, illustrate this behavior. The solid black symbols show data for the 5 ppt ^3He sample. At 600 mK there was essentially no flow, only elastic deformation, and both P_{ac} and $\Delta\phi$ agreed with the “no flow” sample’s purely elastic values. As the temperature was lowered, the flow rate (and therefore P_{ac}) increased.

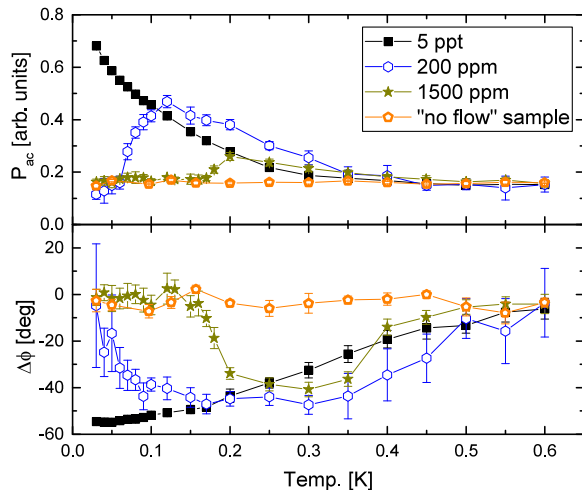


FIG. 4. Temperature dependence of P_{ac} and $\Delta\phi$ measured in ac method for three samples with $x_3 = 5\text{ppt}$, 200 ppm, and 1500 ppm. ac measurement of a sample with no mass flow is also plotted for comparison. Measurements were performed with $f = 0.02$ Hz and $V_0 = 50$ V.

Since flow occurred on a time scale of minutes, the response lagged behind the 0.02 Hz drive, producing a nonzero phase shift $\Delta\phi$. P_{ac} , which reflects the flow rate, continued to increase to the lowest temperature, with no sign of saturation but becoming faster instead. The samples with larger ^3He concentrations (200 and 1500 ppm) showed the same behavior as in the dc measurements of Fig. 3: an increasing pressure response P_{ac} below 600 mK, followed by a drop at a lower temperature. This is clearest for the 1500 ppm sample (brown symbols), where flow is completely suppressed, leaving only the elastic response, so both P_{ac} and $\Delta\phi$ return to the purely elastic values at the lowest temperatures.

Other than the ^3He effects, the flow described in this Letter has essentially the same temperature and pressure dependence as that seen in previous experiments with superfluid Vycor leads (LSL) or a Vycor channel (SLS), strongly suggesting that the same bulk solid flow mechanism is involved. In the samples with extremely low ^3He concentrations (x_3 of 5 ppt and 120 ppb), the flow not only continues but also increases down to at least 28 mK. This behavior rules out vacancy diffusion or other thermally activated processes as the mechanism of mass flow [17,20]. Grain boundaries and dislocations have been suggested as flow paths in ^4He , based on numerical simulations indicating that both may be superfluid [21,22]. Recent measurements in the LSL geometry showed the flow approaching $1/T$ dependence with temperature close to 100 mK [13]. By extending the intrinsic flow to 28 mK, we observed that the increase of flow rate [shown in Fig. 2(b)] is slower than $1/T$.

The absence of low temperature flow suppression in our 120 ppb sample actually supports our earlier conclusion that ^3He blocks mass flow by accumulating at the solid-liquid interfaces in the SLS experiment [12]. If the effect of ^3He in the those experiments was simply to block flow channels within a static network of superfluid dislocation cores, more ^3He than in our current experiment would be needed, since the liquid in the Vycor removes much of the ^3He from the solid at low temperatures. However, we observe the opposite: less ^3He was needed to block flow than in our current experiments with no liquid. For example, in the SLS experiments [12] 120 ppb of ^3He reduced the flow by 67% below 100 mK, but in the present experiments, more than 20 ppm ^3He was needed to achieve similar suppression. Moreover, 20 ppm of ^3He completely blocked the low temperature flow in the SLS experiments while more than 200 ppm was needed in the current measurements. At concentrations for which both bulk solid and SLS samples showed a drop in flow, the temperature at which it occurred was lower for the bulk solid. Table I gives the temperatures at which the drop in flow began (T_{onset}) and ended (T_d), and the maximum amount by which it was reduced, for both the bulk solid samples and the SLS samples.

TABLE I. Temperatures at which the drop in flow began (T_{onset}) and ended (T_d) and the maximum reduction. For each ^3He concentration, the first values are for bulk solid (this work) and the second values (in brackets) are for SLS samples [12]. Dashes indicate samples for which no suppression was observed. “NA” indicates that no measurements were done at that concentration.

x_3 [ppm]	T_{onset} [mK]	T_d [mK]	Reduction
0.001	NA (90)	NA (40)	NA (32%)
0.120	—(100)	—(70)	—(67%)
20	100 (160)	40 (110)	42% (100%)
200	120 (180)	70 (140)	74% (100%)
1500	160 (NA)	100 (NA)	100% (NA)

Figure 5 compares the temperatures T_d for the different flow experiments. The measurements with LSL or SLS junctions had essentially the same values for T_d , suggesting that the ^3He blocked the flow path in the same way when superfluid in Vycor was involved. In the present measurements, the flow drop occurred at lower temperatures. From Fig. 5, we estimate that roughly 2 orders of magnitude more ^3He is needed for bulk samples to have the same T_d as those where Vycor and superfluid are present. This means that if the ^3He is blocking a superfluid flow path, that channel must involve a larger area and/or weaker ^3He binding than the LSL and SLS samples. Quantum Monte Carlo simulations have shown that two-dimensional defects like grain boundaries can be superfluid in solid ^4He [21]. Similar calculations for disordered layers adjacent to walls also found that ^3He atoms bind to this layer at low temperatures and suppress its superfluidity [18], confirmed by specific heat measurements with solid ^4He grown in porous glass [23]. The surface area of the cell walls for our solid sample, 1162 mm², is more than 50 times larger than that of the solid-liquid interfaces (21.5 mm²) at the ends of the Vycor rods in the SLS samples. This ratio will be even larger considering grain boundaries in polycrystalline samples, which could be why much larger ^3He concentrations are needed to block the flow.

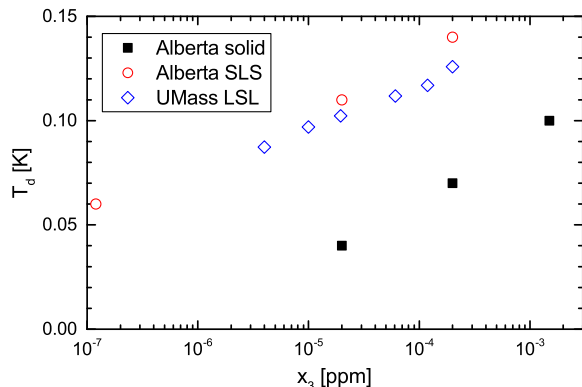


FIG. 5. T_d versus x_3 . The “Alberta SLS” data are taken from Ref. [12] and the “UMass LSL” data from Ref. [10].

Indeed, the number of atoms in a surface or a few grain boundaries is too small to produce the observed pressure changes, and the flow in 2D Kosterlitz-Thouless superfluids should be constant at low temperatures [24,25]. This suggests that such layers could be conduits for flow but not the source of the mass being transported. Mass would have to be injected from the solid at the compressed end of a flow channel and back into the solid at the other end. This “syringe effect” is possible if dislocations can propagate and proliferate within the solid via superclimb, as described in recent papers [26–28]. The observed temperature dependence of the flow could then reflect the rate of this process, rather than the flow within a liquid channel itself. In conventional crystals, climb allows dislocations to move past pinning sites. So, although requiring superfluid cores, superclimb may still be an effective mass transport mechanism within solid helium even in the presence of ^3He impurities.

The measurements described above clearly show that mass flow in solid helium does not require superfluid leads but can be generated directly by pressure differences created by mechanical compression in bulk solids. The flow that appears below 600 mK is not thermally activated—its rate increases as the temperature decreases. The flow rate is not proportional to the pressure difference across the solid but rather continues at a high rate and then stops rather abruptly when the final pressure is reached after a few minutes. This behavior is more typical of superflow than of a viscous liquid or conventional plastic flow. We were able to eliminate the effects of ^3He impurities by using ^4He with extremely high isotopic purity, and found that the flow rate in the solid continued to increase down to at least 28 mK. We also added ^3He and found the same qualitative behavior as in earlier experiments with Vycor superfluid channels. However, much more ^3He was needed to block the flow, indicating that the flow path involved a larger area and/or weaker binding of ^3He in the current experiments. Possibilities for the flow path include disordered layers near the cell walls and grain boundaries.

We thank S. Balibar for providing the extremely isotopically pure ^4He gas. This work was supported by a grant from NSERC Canada.

- [1] A. F. Andreev and I. M. Lifshitz, *Sov. Phys. JETP* **29**, 1107 (1969).
- [2] A. J. Leggett, *Phys. Rev. Lett.* **25**, 1543 (1970).
- [3] G. Chester, *Phys. Rev. A* **2**, 256 (1970).
- [4] E. Kim and M. H. W. Chan, *Nature (London)* **427**, 225 (2004).
- [5] E. Kim and M. H. W. Chan, *Science* **305**, 1941 (2004).
- [6] J. R. Beamish, A. D. Fefferman, A. Haziot, X. Rojas, and S. Balibar, *Phys. Rev. B* **85**, 180501 (2012).
- [7] H. J. Maris, *Phys. Rev. B* **86**, 020502 (2012).

- [8] D. Y. Kim and M. H. W. Chan, *Phys. Rev. Lett.* **109**, 155301 (2012).
- [9] M. W. Ray and R. B. Hallock, *Phys. Rev. Lett.* **100**, 235301 (2008).
- [10] Y. Vekhov, W. J. Mullin, and R. B. Hallock, *Phys. Rev. Lett.* **113**, 035302 (2014).
- [11] E. B. Molz and J. R. Beamish, *J. Low Temp. Phys.* **101**, 1055 (1995).
- [12] Z. G. Cheng, J. Beamish, A. D. Fefferman, F. Souris, S. Balibar, and V. Dauvois, *Phys. Rev. Lett.* **114**, 165301 (2015).
- [13] Y. Vekhov and R. B. Hallock, *Phys. Rev. B* **91**, 180506 (2015).
- [14] [http://www.piceramic.com/Model 141-03](http://www.piceramic.com/Model%20141-03).
- [15] The 5 ppt ^4He gas was purified by P. McClintock at Lancaster University and provided by S. Balibar at ENS. The ^3He concentration was analyzed by K. A. Farley at California Institute of Technology.
- [16] See Supplemental Material at <http://link.aps.org/supplemental/10.1103/PhysRevLett.117.025301>, which includes Refs. [14,17–19], for design of experimental cell, estimation of elastic response, calculation for fully hydrodynamic relaxation, details of ac measurements, and calculation of ^3He distribution.
- [17] A. Suhel and J. R. Beamish, *Phys. Rev. B* **84**, 094512 (2011).
- [18] S. A. Khairallah and D. M. Ceperley, *Phys. Rev. Lett.* **95**, 185301 (2005).
- [19] J. Beamish, *J. Low Temp. Phys.* **168**, 194 (2012).
- [20] A. Lisunov, V. Maidanov, N. Mikhin, A. Neoneta, V. Rubanskyi, S. Rubets, E. Rudavskii, and V. Zhuchkov, *J. Low Temp. Phys.* **175**, 113 (2014).
- [21] L. Pollet, M. Boninsegni, A. B. Kuklov, N. V. Prokof'ev, B. V. Svistunov, and M. Troyer, *Phys. Rev. Lett.* **98**, 135301 (2007).
- [22] M. Boninsegni, A. B. Kuklov, L. Pollet, N. V. Prokof'ev, B. V. Svistunov, and M. Troyer, *Phys. Rev. Lett.* **99**, 035301 (2007).
- [23] Z. G. Cheng, N. Mulders, and M. H. W. Chan, *Phys. Rev. B* **90**, 224101 (2014).
- [24] M. W. Toft and J. G. M. Armitage, *J. Low Temp. Phys.* **52**, 343 (1983).
- [25] G. Agnolet, D. F. McQueeney, and J. D. Reppy, *Phys. Rev. B* **39**, 8934 (1989).
- [26] S. G. Söyler, A. B. Kuklov, L. Pollet, N. V. Prokof'ev, and B. V. Svistunov, *Phys. Rev. Lett.* **103**, 175301 (2009).
- [27] A. B. Kuklov, *Phys. Rev. B* **92**, 134504 (2015).
- [28] A. B. Kuklov, L. Pollet, N. V. Prokof'ev, and B. V. Svistunov, *Phys. Rev. B* **90**, 184508 (2014).